

# The Structural Influence on the Rashba-type Spin-Splitting in Surface Alloys

Isabella Gierz,<sup>1,\*</sup> Benjamin Stadtmüller,<sup>1,2,†</sup> Johannes Vuorinen,<sup>3</sup> Matti Lindroos,<sup>3</sup> Fabian Meier,<sup>4,5</sup> J. Hugo Dil,<sup>4,5</sup> Klaus Kern,<sup>1,6</sup> and Christian R. Ast<sup>1</sup>

<sup>1</sup>Max-Planck-Institut für Festkörperforschung, 70569 Stuttgart, Germany

<sup>2</sup>Physikalisches Institut, Universität Würzburg, 97074 Würzburg, Germany

<sup>3</sup>Tampere University of Technology, Department of Physics, 33101 Tampere, Finland

<sup>4</sup>Physik-Institut, Universität Zürich, 8057 Zürich, Switzerland

<sup>5</sup>Swiss Light Source, Paul Scherrer Institute, 5232 Villigen, Switzerland

<sup>6</sup>IPMC, Ecole Polytechnique Fédérale de Lausanne, 1015 Lausanne, Switzerland

(Dated: October 17, 2021)

The Bi/Ag(111), Pb/Ag(111), and Sb/Ag(111) surface alloys exhibit a two-dimensional band structure with a strongly enhanced Rashba-type spin-splitting, which is in part attributed to the structural asymmetry resulting from an outward relaxation of the alloy atoms. In order to gain further insight into the spin-splitting mechanism, we have experimentally determined the outward relaxation of the alloy atoms in these surface alloys using quantitative low-energy electron diffraction (LEED). The structure plays an important role in the size of the spin-splitting as it dictates the potential landscape, the symmetry as well as the orbital character. Furthermore, we discuss the band ordering of the Pb/Ag(111) surface alloy as well as the reproducible formation of Sb/Ag(111) surface alloys with unfaulted (face-centered cubic) and faulted (hexagonally close-packed) toplayer stacking.

## INTRODUCTION

The Rashba-Bychkov (RB) model has been remarkably successful in describing two-dimensional (2D) electron systems with a structural inversion asymmetry (SIA). It describes how an electric field perpendicular to the 2D electron system lifts the spin-degeneracy resulting in a characteristic band dispersion [1]. Originally developed for semiconductor heterostructures, it has also been successfully applied to surface states on various surfaces even though the boundary conditions are different than for the heterostructures [2]. Extending the RB model to include an in-plane potential gradient coming from a lattice potential with an in-plane inversion asymmetry, results in a strong enhancement of the spin-splitting [3].

The spin-splitting mechanism relies on different contributions, such as a strong spin-orbit interaction, a SIA as well as other structural parameters (e. g., corrugation, relaxation, orbital character) [4–9]. The RB model can as such only serve as a qualitative model because it only accounts for an effective electric field acting on a 2D free electron gas, which combines all these different contributions in one single parameter. The importance of detailed structural considerations, which are completely neglected in the framework of the RB model in the nearly free electron gas, becomes obvious when comparing silver and antimony. Ag and Sb atoms are of about the same size and exhibit a very similar atomic spin-orbit coupling. The surface states on the (111) surfaces of these elements, however, exhibit substantially different spin-splittings, the one in Ag(111) being much smaller than in Sb(111) [7, 10, 11]. Since surface potential gradient and atomic spin-orbit coupling can be considered to be of the same order of magnitude, the reason for this difference in spin-splitting must be sought in the structure. The face-centered-cubic structure of Ag features a smooth hexagonal lattice at the (111) surface, whereas the rhombohedral structure of Sb(111) with two atoms in the basis grows in a bilayer configuration stacked along the [111]

direction resulting in a corrugated surface [12]. Hence, structural considerations have to be taken into account for a better understanding of the Rashba-type spin-splitting in surface states. For systems with a similar crystal structure like Bi and Sb the different size of the spin-splitting can be attributed to the difference in atomic mass [10, 13, 14]. Further, even though the atomic spin-orbit coupling is vanishingly small in graphene or carbon nanotubes, it has been shown that the spin-orbit interaction can be structurally enhanced by the local curvature in their structure [9, 15, 16].

Recently a number of surface alloys (Bi/Ag(111), Pb/Ag(111), etc.) have been identified with an extremely large spin-splitting in the electronic structure at the surface [17–21]. Interestingly, only a fraction of the atoms at the surface feature a sizeable atomic spin-orbit coupling so that here as well the source of the large spin-splitting must be sought in the structure. Motivated by this and by theoretical considerations about the relaxation dependence of the spin-splitting [6] we present a systematic study of the alloy atom relaxation in different Ag(111) surface alloys using quantitative low-energy electron diffraction (IV-LEED) measurements and calculations. We relate the dopant atom relaxation to the size of the spin-splitting and address a number of other unresolved issues in the literature. These include the band assignment of the bands crossing the Fermi level in the Pb/Ag(111) surface alloy, hcp (hexagonal close-packed) and fcc (face-centered cubic) toplayer stacking in the Sb/Ag(111) surface alloy as well as the Bi atom relaxation in the Ag(111) and Cu(111) surface alloys.

## EXPERIMENTS AND CALCULATIONS

All experiments were performed in ultra high vacuum (UHV) with a base pressure of  $1 \times 10^{-10}$  mbar at 77 K. The angular resolved photoemission spectroscopy (ARPES)

measurements were done with a SPECS HSA3500 hemispherical analyzer with an energy resolution of 10 meV and monochromatized HeI radiation. The IV-LEED measurements were done using an ErLEED 1000-A. During IV-LEED measurements magnetic stray fields were compensated using Helmholtz coils to assure perpendicular incidence of the electrons on the sample for all kinetic energies. The Ag(111) substrate was cleaned using several sputtering/annealing cycles. Cleanliness of the substrate was checked with X-ray photoemission spectroscopy (XPS) and the different surface states were controlled with ARPES. One third of a monolayer (ML) of Bi, Pb, or Sb (henceforth referred to as alloy atoms) was deposited using a commercial electron beam evaporator. The substrate temperature during deposition was 420°C, 350°C, and 250°C for Bi, Pb and Sb, respectively.

We performed IV-LEED calculations using the experimental data for Bi/Ag(111), Pb/Ag(111) and two different measurements for Sb/Ag(111). For each of the four experimental data sets both the unfaulted (fcc) substitutional and the faulted (hcp) substitutional structures were calculated. For all structures the decision between fcc and hcp toplayer stacking was very clear as the Pendry  $R_P$ -factors for the rejected structures were in all cases more than double to those of the correct structures.

During the calculations surface geometry, Debye temperatures and real part of the inner potential were optimized. In every set the geometry of the four highest layers was calculated as a  $(\sqrt{3} \times \sqrt{3})$  unit cell. The symmetry restricts the degrees of freedom to the component normal to the surface and also forbids buckling for most layers. Three Debye temperatures  $T_D$  were fitted for each measurement, the top layer Ag atoms, top layer Pb/Bi/Sb atoms and of all the other Ag atoms. The real part of the inner potential was optimized and found to be approximately 6 eV for all calculations. The imaginary part of the potential was kept at a fixed value of 4.5 eV for all calculations.

The LEED calculations were performed using the Barbieri/Van Hove SATLEED package [22]. The necessary fourteen phase shifts were determined with the Barbieri/Van Hove phase shift package [23]. Temperature effects were calculated within the SATLEED code by multiplying each atoms scattering amplitude by a Debye-Waller factor. Pendry  $R_P$ -factors [24] were used to measure the level of agreement between measured and calculated IV-LEED spectra and statistical errors in analysis were estimated with Pendry RR-factors [24].

## RESULTS AND DISCUSSION

Although (Bi, Pb, Sb) and Ag are immiscible in the bulk, they form a long-range ordered surface alloy where every third Ag atom in the topmost layer is replaced by an alloy atom. The resulting  $(\sqrt{3} \times \sqrt{3})R30^\circ$  structure (with respect to the pristine Ag(111) surface) is displayed in Fig. 1 a). The alloy atoms relax out of the plane of the Ag layer by an amount  $\Delta z$  as shown in the side view in Fig. 1 a) [6, 17, 18, 25, 26].

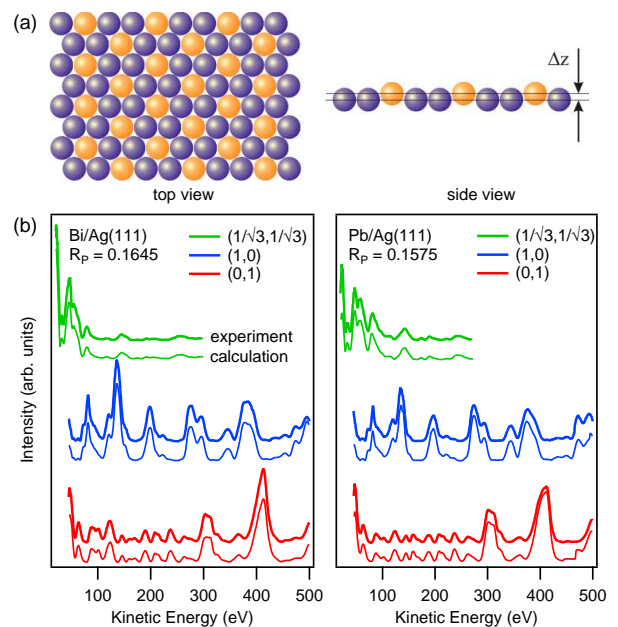


FIG. 1: (color online) Panel (a) shows the top and side views for the  $(\sqrt{3} \times \sqrt{3})R30^\circ$  structure formed by the surface alloys on Ag(111). Ag atoms are shown in red, alloy atoms are shown in blue. The outward relaxation of the alloy atoms is defined as the vertical distance between alloy and Ag atoms in the topmost layer. In Panel (b) IV-LEED data (thick lines) for the  $(\sqrt{3} \times \sqrt{3})R30^\circ$  phase of Bi (left) and Pb (right) on Ag(111) are displayed together with the corresponding calculated IV-LEED spectra (thin lines).

Fig. 1 b) shows the integrated intensity of the (0,1), (1,0), and  $(1/\sqrt{3}, 1/\sqrt{3})$  spots as a function of electron energy for the Bi/Ag(111) and Pb/Ag(111) surface alloys. The data were averaged over three (six) equivalent spots and smoothed. The IV-LEED spectra for both Bi/Ag(111) and Pb/Ag(111) surface alloys differ only in detail indicating that they form the same  $(\sqrt{3} \times \sqrt{3})R30^\circ$  structure. For the Sb/Ag(111) surface alloy two different phases are known from the literature, which differ in the toplayer stacking [27–29]. One phase grows in regular face-centered cubic (fcc) stacking while the other phase grows in hexagonal close-packed (hcp) stacking. The IV-LEED spectra for the two Sb/Ag(111) surface alloys, which have been treated in analogy to the spectra in Fig. 1 b), are shown in Fig. 2 a). The thick and thin lines in the graphs correspond to the experimental and calculated spectra, respectively. It can be seen that for all surface alloys the calculated spectra fit very well to the experimental data resulting in low  $R_P$ -factors. Only the  $R_P$ -factor for the hcp-phase of the Sb/Ag(111) is somewhat higher, which we attribute to some fcc-domains being present at the surface.

The structural parameters resulting from the calculated IV-LEED spectra are summarized in Table I along with some values from the literature for comparison. The outward relaxation  $\Delta z$ , which is the distance between the alloy atom and the plane of the first layer of substrate atoms (see Fig. 1b), is given for each of the different alloy atoms. In addition, the

TABLE I: Geometrical parameters of the different surface alloys on Ag(111) and Cu(111) substrates. The outward relaxation  $\Delta z$  is the distance between the alloy atom and the plane of the surface layer. The distances  $d_{12}$ ,  $d_{23}$ , and  $d_{34}$  are the distances between the first (= surface) and second layer, the second and third layer, as well as the third and fourth layer, respectively. The bulk interlayer distances are 2.36 Å for Ag(111) and 2.09 Å for Cu(111).

	geometry	$\Delta z$ (Å)	$d_{12}$ (Å)	$d_{23}$ (Å)	$d_{34}$ (Å)	$R_P$	Ref.	
<b>Bi/Ag(111)</b>	substitutional	$0.65 \pm 0.10$	$2.32 \pm 0.02$	$2.33 \pm 0.03$	$2.34 \pm 0.04$	0.1645	this work	
		0.35 (theory)					[13]	
		0.85 (theory)					[6]	
<b>Pb/Ag(111)</b>	substitutional	$0.46 \pm 0.06$	$2.35 \pm 0.02$	$2.33 \pm 0.03$	$2.34 \pm 0.04$	0.1575	this work	
		0.24 (XRD)					[25]	
		0.8 (STM)					[25]	
		0.68 (theory)					[25]	
		0.42 (theory)					[18]	
<b>Sb/Ag(111)</b>	hcp substitutional	$0.11 \pm 0.05$	$2.43 \pm 0.05$	$2.34 \pm 0.05$	$2.35 \pm 0.06$	0.2548	this work	
		$0.03 \pm 0.07$ (XRD)					$2.50 \pm 0.03$	[34]
		0.02 (theory)					[27]	
		0.07 (LEED)					[28]	
<b>Sb/Ag(111)</b>	substitutional	$0.10 \pm 0.02$	$2.44 \pm 0.02$	$2.33 \pm 0.02$	$2.33 \pm 0.03$	0.1395	this work	
		0.24 (theory)					[20]	
<b>Bi/Cu(111)</b>	substitutional	$1.02 \pm 0.02$ (XRD)	$2.12 \pm 0.01$	$2.10 \pm 0.01$			[37]	
		1.06 (theory)			[38]			
<b>Sb/Cu(111)</b>	hcp substitutional	$0.47 \pm 0.16$ (MEIS)	$2.05 \pm 0.09$				[35]	
		$0.6 \pm 0.03$ (XRD)		$1.98 \pm 0.02$	[34]			

interlayer distances for the first four layers are summarized. After the fourth layer no significant deviation from the bulk value of 2.36 Å is expected. The in-plane lattice constants were held fixed. While for the Pb/Ag(111) and Bi/Ag(111) surface alloys the interlayer distances hardly differ from the bulk, it should be noted that in the Sb/Ag(111) surface alloy the distance between the first and the second silver layer is increased by about 0.1 Å. Furthermore, non-structural parameters that accompany the IV-LEED calculations such as the Debye temperatures as well as the real part of the inner potential are given in Table II. As the IV-LEED measurements were done at 77 K, which is comparable to the low Debye temperatures, no complications from a too high Debye-Waller factor were anticipated in the calculations.

In the following, we relate the structural findings to the size of the Rashba-type spin-splitting. The RB model is described by the Hamiltonian:

$$\hat{H}_{SO} = \alpha_R \boldsymbol{\sigma} \cdot (\mathbf{k}_{\parallel} \times \mathbf{e}_z) \quad (1)$$

where  $\alpha_R$  is the Rashba parameter. The resulting energy dispersion in the nearly free electron model is  $E(\mathbf{k}_{\parallel}) = \frac{\hbar^2}{2m^*} (k_{\parallel} \pm k_0)^2 + E_0$  where  $m^*$  is the effective mass,  $k_0 = m^* \alpha_R / \hbar^2$  is the offset by which the parabola is shifted away from the high symmetry point, and  $E_0$  is an offset in energy. The Rashba energy  $E_R = \hbar^2 k_0^2 / 2m^*$  is the energy difference between the band extremum and the crossing point at the high symmetry point. The three parameters  $k_0$ ,  $\alpha_R$ , and  $E_R$  quantify the strength of the Rashba-type spin-splitting and serve

well to compare the different spin-split bands in the surface alloys. An overview of the typical parameters in these systems is given in Table III.

### Bi/Ag(111)

With  $\Delta z = 0.65 \pm 0.10$  Å, the Bi/Ag(111) surface alloy shows the largest outward relaxation in the surface alloys considered here on a Ag(111) substrate. So far only two theoretical values have been reported for the relaxation, one of which is smaller while the other is larger than the experimental value (see Table I). The difference between the theoretical values is most likely related to different methods for relaxing the structure. Nevertheless, the corresponding band structure calculations both show good agreement with the experimental data [6, 18].

Calculations have shown that an increased  $p_{xy}$ -character in the fully occupied band is responsible for the enhanced spin-splitting characterized by a momentum offset of  $k_0 = 0.12$  Å<sup>-1</sup> in Bi/Ag(111) [6]. It was shown that starting from a hypothetical flat Bi/Ag(111) surface alloy the  $s : p_z$ -ratio changes in favor of the  $p_z$ -character with an admixture of  $p_{xy}$ -character upon outward relaxation of the Bi atoms resulting in a stronger spin-splitting. Comparing the Bi/Ag(111) surface alloy to the Bi/Cu(111) surface alloy, we find that the structure is qualitatively the same for both surface alloys. However, for the Bi/Cu(111) surface alloy outward relaxations of more

TABLE II: Non structural parameters that have been used in the IV-LEED calculation. The Debye temperatures  $T_D$  for the different alloy atoms (Pb/Bi/Sb), the surface layer silver atoms ( $\text{Ag}_1$ ), and the silver atoms in the subsequent layers ( $\text{Ag}_{2\rightarrow}$ ) are given along with the real part of the inner potential  $V_R$ .

	$T_D(\text{Pb/Bi/Sb})(\text{K})$	$T_D(\text{Ag}_1)(\text{K})$	$T_D(\text{Ag}_{2\rightarrow})(\text{K})$	$V_R(\text{eV})$
<b>Pb/Ag(111)</b>	90	150	180	6.3
<b>Bi/Ag(111)</b>	65	160	210	5.9
<b>Sb/Ag(111) hcp subst.</b>	150	110	230	5.7
<b>Sb/Ag(111) subst.</b>	115	130	200	6.2

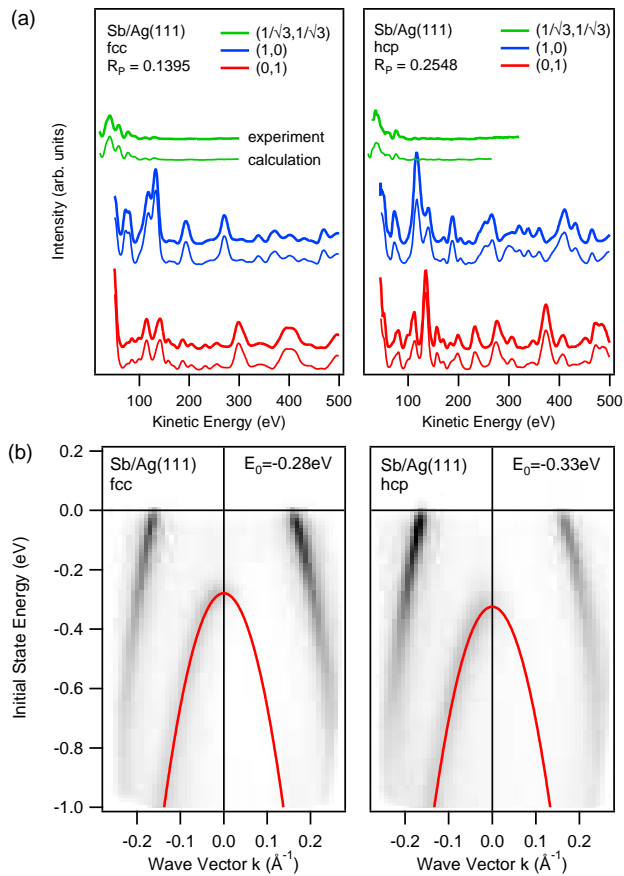


FIG. 2: (color online) Comparison of IV-LEED (a) and ARPES (b) data for fcc (left panels) and hcp (right panels) toplayer stacking for the Sb/Ag(111) surface alloys. The red lines in b) are fits to the experimental data.

than one Ångström have been reported (see Table I). The difference in outward relaxation can be attributed to the smaller lattice constant of the Cu substrate. A comparison of the electronic structures shows that the spin-splitting  $k_0 = 0.03 \text{ \AA}^{-1}$  for Bi/Cu(111) is much smaller than for Bi/Ag(111). Furthermore, the surface alloy bands in Bi/Cu(111) are shifted into the unoccupied states, which can be related to a different charge transfer to the surface state from the Cu bulk as compared to the Ag bulk.

TABLE III: Characteristic parameters for the spin-split states in the different surface alloys on the Ag(111) and Cu(111) surfaces. The different parameters, momentum offset  $k_0$ , Rashba energy  $E_R$ , and Rashba constant  $\alpha_R$  are defined in the text.

System	$k_0 (\text{Å}^{-1})$	$E_R (\text{meV})$	$\alpha_R (\text{eVÅ})$	Ref.
Sb/Ag(111)	0.005	5.7	0.76	[20, 36]
Pb/Ag(111)	0.03	23	1.52	[19] (exp)
	0.04	22	1.05	[19] (theor)
	0.11			[6]
Bi/Ag(111)	0.13	200	3.05	[18]
	0.13			[6]
Sb/Cu(111)	0.005	3	0.19	[40]
Bi/Cu(111)	0.03	15	1.0	[21]
	0.096			[41]
	0.032	13	0.82	[38] (exp)
	0.028	9	0.62	[38] (theor)
Au(111)	0.012	2.1	0.33	[42]
Ag(111)	0.0007	0.005	0.013	[7]
Cu(111)	0	0	0	[43]

### Pb/Ag(111)

For the Pb/Ag(111) surface alloy an outward relaxation of  $\Delta z = 0.46 \pm 0.06 \text{ \AA}$  has been found. This value lies in between previously reported values excluding the value obtained by scanning tunneling microscopy (STM). STM is generally not very suitable for obtaining structural parameters perpendicular to the surface [25]. Also, in contrast to what has been observed before [25], our IV-LEED calculations show that the two lattice sites of the Ag atoms in the  $\sqrt{3} \times \sqrt{3} R30^\circ$  unit cell are equivalent.

The size of the spin-splitting for the Pb/Ag(111) surface alloy is still under debate due to different interpretations of the measured ARPES spectra [6, 30–32]. Depending on the band dispersion of the  $sp_z$ -band and the  $p_{xy}$ -band in the unoccupied states, the occupied states may be assigned to different bands [6, 18]. It has been shown that the position of the  $sp_z$ -band is particularly sensitive to the outward relaxation of the Pb atoms [6]. With a calculated outward relaxation of  $0.97 \text{ \AA}$ , the  $sp_z$ -band with  $k_0 = 0.11 \text{ \AA}^{-1}$  and the  $p_{xy}$ -band cross without hybridizing (Scenario I). By reducing the relaxation of the Pb atoms to  $0.67 \text{ \AA}$ , however, the two sets of bands avoid each

other resulting in a lower apparent spin-splitting (Scenario II) [6]. Other calculations found a relaxation of  $0.42 \text{ \AA}$  leading to a spin-splitting of  $0.04 \text{ \AA}^{-1}$  in good agreement with experiment [19, 33]. Here, no band crossing between the  $sp_z$ -band and the  $p_{xy}$ -band has been observed. As the experimental outward relaxation found for Pb/Ag(111) is  $0.46 \text{ \AA}$ , we are inclined to favor the second scenario. This interpretation is further supported by recent spin-resolved ARPES measurements [32].

### Sb/Ag(111)

The Sb/Ag(111) surface alloy can be formed with either fcc or hcp toplayer stacking [27, 29]. However, no reproducible way of creating these two phases has been reported so far. The formation of the hcp toplayer stacking has been attributed to the presence of subsurface stacking faults from previous preparations caused by Sb atom diffusion into the bulk [27]. We have found that it is possible to reproducibly create the two phases separately regardless of the sample preparation history. In the electron beam evaporator used for depositing the Sb atoms, the atom beam is partially ionized by electrons from a filament. A positive voltage at the crucible accelerates the Sb ions towards the grounded sample. The higher the voltage at the crucible, the higher the kinetic energy of the Sb ions and therefore the stronger their impact at the Ag(111) surface. For voltages below  $+370 \text{ V}$  at the Sb crucible as well as for thermal Sb atoms evaporated from a Knudsen cell, we found that the phase with fcc-stacking is formed. For higher voltages the phase with hcp-stacking is formed. It is conceivable that the higher ion energy results in ion implantation into the Ag substrate inducing the subsurface stacking faults that favor the phase with hcp-stacking.

The Sb outward relaxation for the fcc- and hcp-phase is  $0.1 \pm 0.02 \text{ \AA}$  and  $0.11 \pm 0.05 \text{ \AA}$ , respectively. These values are similar to what has been previously found for the hcp-phase using IV-LEED. In addition, a slight outward relaxation between  $0.07 \text{ \AA}$  and  $0.08 \text{ \AA}$  of the surface Ag layer has been observed for both phases. The Ag layer relaxation has also been found by x-ray diffraction (XRD). There the Ag layer relaxation is larger ( $0.14 \text{ \AA}$ ), whereas the outward relaxation of the Sb atom is smaller ( $0.03 \text{ \AA}$ ) [34]. A similar effect has been observed for the Sb/Cu(111) surface alloy. There, however, the Cu layer relaxation reduces the distance between the surface layer and the substrate [34, 35].

The toplayer stacking also slightly affects the band structure. This can be seen in Fig. 2(b), where the experimental band structure of the two phases for the Sb/Ag(111) surface alloy in the vicinity of the  $\bar{\Gamma}$ -point is shown. We observe a small shift of  $50 \text{ meV}$  between the  $sp_z$ -band of the two phases. However, due to the comparatively large error bars we cannot relate this to the outward relaxation. We rather attribute this shift to possible disorder at the surface. This interpretation is also supported by the larger  $R_P$ -factor for the hcp-phase.

The spin-splitting of the  $sp_z$ -band is too small to be detected

by conventional ARPES. However, spin-resolved photoemission experiments, which are much more sensitive to a small spin-splitting due to the “spin-label” of the bands [32], show that the  $sp_z$ -band of the hcp-phase in the Sb/Ag(111) surface alloy is spin-split by  $0.005 \text{ \AA}^{-1}$  [36]. Unfortunately, no spin-splitting has been reported so far for the fcc-phase.

### Spin-splitting vs. Relaxation

The large spin-splitting in the different surface alloys cannot be accounted for by the spin-orbit interaction in the heavy elements alone. This becomes obvious when comparing them to other materials with a sizeable spin-splitting, such as Au(111) or Bi(111). The spin-splitting of the surface state on the pristine Ag(111) substrate is experimentally undetectable with current experimental techniques. The spin-splitting in the Bi/Ag(111) surface alloy is much larger than what has been observed for the Bi(111) surface state, even though only a fraction of the atoms in the surface alloy are Bi atoms. Thus, the simple statement that a strong spin-orbit coupling leads to a large spin-splitting does not hold.

In order to resolve this issue the structural details of the different materials have to be considered. As the structure dictates the potential landscape, the orbital overlap as well as the orbital hybridization, it has direct influence on the asymmetry of the wave functions and the corresponding spin-splitting in the electronic structure. In Fig. 3a–c the characteristic parameters for the Rashba-type spin-splitting in the different surface alloys — momentum offset  $k_0$ , Rashba energy  $E_R$ , and Rashba constant  $\alpha_R$  — are plotted as a function of the outward relaxation. The surface alloys on the Cu(111) and the Ag(111) substrates are drawn in blue squares and red circles, respectively. The solid lines are drawn to guide the eye.

Unfortunately, with experimentally available systems it is difficult to change only one parameter, while leaving everything else constant. Nevertheless, the available data allows us to define some trends. A schematic of the different parameter changes is shown in Fig. 3d for the four different systems that are known on a Ag(111) substrate. The bare Ag(111) surface state has been included as a reference point with no outward relaxation. The other three surface alloys are arranged such that the parameter changes become apparent. Along the horizontal direction, from left to right the outward relaxation changes, but the mass of the elements (Ag  $\rightarrow$  Sb; Pb  $\rightarrow$  Bi) remains almost the same. Along the vertical direction, the outward relaxation changes along with the atomic spin-orbit coupling as the atomic mass changes by a factor of almost two (Ag  $\rightarrow$  Pb; Sb  $\rightarrow$  Bi).

With the schematic in Fig. 3d in mind, the general trend that an increased spin-orbit coupling and an increased outward relaxation leads to an increased spin-splitting seems to be evident, when considering the Ag(111) and the Cu(111) substrates separately. If we consider that the atomic spin-orbit coupling constant for  $p$ -electrons in a hydrogen-like atom is proportional to  $Z^4/n^3$  ( $Z$ : atomic number,  $n$ : principal quan-

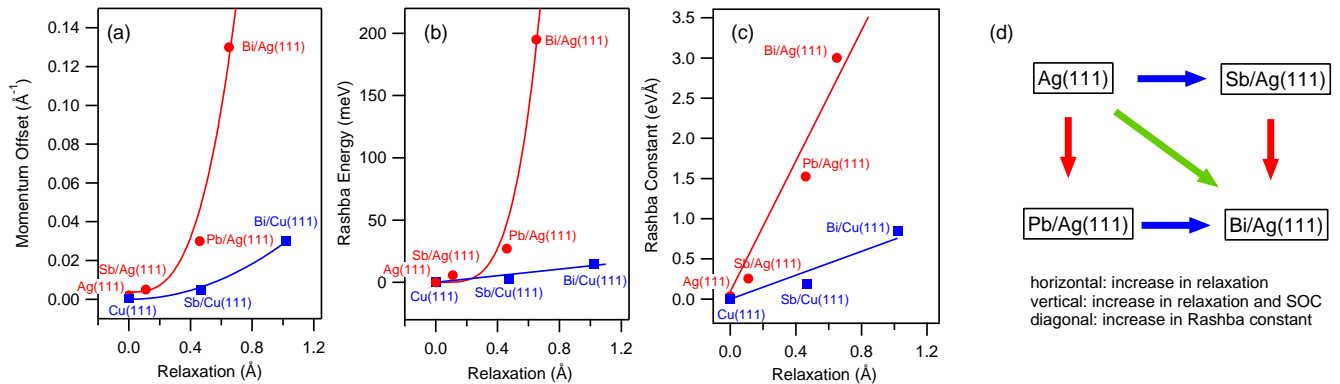


FIG. 3: (color online) Characteristic experimental parameters for a Rashba system, such as momentum offset (a), Rashba Energy (b), and Rashba constant are shown as a function of the outward relaxation  $\Delta z$ . The lines are drawn as a guide to the eye. In (d) a schematic of the evolution of the outward relaxation and the atomic spin-orbit coupling is drawn for the different surface alloys.

tum number), the increase in the atomic spin-orbit coupling constants of Sb, Pb, and Bi alone cannot account for the increase in the respective Rashba constants. Therefore, we conclude that the structure of the surface alloy, i. e. the outward relaxation, plays a key role in the strength of the spin-splitting.

Comparing the surface alloys for the Ag(111) and Cu(111) substrates, the situation is not so straightforward anymore. The Bi/Cu(111) surface alloy shows a much larger outward relaxation, but a much smaller spin-splitting than the Bi/Ag(111) surface alloy. It is conceivable that the substrate itself has an influence on the size of the spin-splitting. Calculations for the  $sp_z$ -states have shown that the substrate atoms within the surface alloy layer carry a significant spectral weight, which has led to the conclusion that the atomic spin-orbit parameter of the substrate contributes to the spin-splitting in the corresponding surface alloys [21]. However, in another comparison of the Bi/Ag(111) and the Bi/Cu(111) surface alloy, the spin-orbit coupling of the substrate has been found to play a negligible role in the spin-splitting of the surface alloy. The conclusion here was that structural effects (i. e. the outward relaxation of the alloy atom) changing the orbital composition play a dominant role [38]. The difference between Bi/Ag(111) and Bi/Cu(111) could simply originate from the different lattice constants of the substrate. In this regard, a simple tight-binding calculation shows that the Rashba constant is proportional to the lattice constant [39]. Another possible explanation is that the spin-splitting reaches a maximum with further outward relaxation leading to smaller spin-splitting. In addition, the distance  $d_{12}$  between the surface layer and the substrate is compressed for Bi/Ag(111) and expanded for Bi/Cu(111) with respect to the bulk interlayer spacing. Whether this plays a role in the spin-splitting for the surface alloys so far is unknown.

The results discussed here show that the outward relaxation plays a key role in the size of the spin-splitting in the surface alloys with the general trend that a larger outward relaxation leads to a larger spin-splitting. However, many open ques-

tions remain, such as a better understanding of the role of the substrate, the influence of avoided crossings of the bands and the resulting apparent spin-splittings as well as the question whether there is a maximum in outward relaxation after which the spin-splitting decreases again.

## CONCLUSION

We have experimentally determined the outward relaxation of the alloy atoms for three different surface alloys (Bi/Ag(111), Pb/Ag(111) and Sb/Ag(111)) employing quantitative LEED measurements and calculations. The outward relaxation for Pb/Ag(111) is 0.46 Å, which leads us to favor the second scenario with the smaller spin-splitting. In addition, we found that the Sb/Ag(111) surface alloy can be grown reproducibly in fcc- and hcp-toplayer stacking. Furthermore, we have related the outward relaxation to the strongly enhanced spin-splitting in the Ag(111) surface alloys comparing them also to surface alloys found on Cu(111). We find that the outward relaxation plays an extremely important role in the size of the spin-splitting, because the ratio of the spin-orbit coupling strengths alone does not account for the ratio of the Rashba constants in two different surface alloys. Looking at each substrate individually a clear trend that a large outward relaxation leads to a large spin-splitting is evident. Deviations from this trend can be observed when comparing the surface alloys on two different substrates, e. g. Bi/Ag(111) and Bi/Cu(111). This could be explained by the different orbital composition in the surface alloy band structure. The role of the substrate has not been completely solved yet.

We conclude that the structure plays an important role in the spin-splitting as it defines the potential landscape and has a profound influence on the orbital overlap and the band dispersion. This has also been found for graphene as well as carbon nanotubes where the atomic spin-orbit interaction is clearly small. Nevertheless, a straightforward, intuitive model

for a better understanding of the Rashba-type spin-splitting at surfaces would be desirable — if it exists.

### ACKNOWLEDGMENTS

We would like to thank U. Starke for help with the IV-LEED measurements as well as H. M. Benia for stimulating discussions. C. R. A. acknowledges funding from the Emmy-Noether-Program of the Deutsche Forschungsgemeinschaft (DFG).

---

\* Corresponding author; electronic address: i.gierz@fkf.mpg.de

† Present address: Institute of Bio- and Nanosystems (IBN-3) and JARA-Fundamentals of Future Information Technologies, Research Center Jülich, 52425 Jülich, Germany

- [1] Y. A. Bychkov and E. I. Rashba, *Sov. Phys. JETP Lett.* **39**, 78 (1984)
- [2] S. LaShell, B. A. McDougall and E. Jensen, *Phys. Rev. Lett.* **77**, 3419 (1996)
- [3] J. Prempfer, M. Trautmann, J. Henk and P. Bruno, *Phys. Rev. B* **76**, 073310 (2007)
- [4] L. Petersen and P. Hedegård, *Surf. Science* **459** 49 (2000)
- [5] J. Henk, A. Ernst, P. Bruno, *Phys. Rev. B* **68**, 165416 (2003)
- [6] G. Bihlmayer, S. Blügel and E. V. Chulkov *Phys. Rev. B* **75** 195414 (2007)
- [7] F. Reinert, *J. Phys.: Cond. Mat.* **15**, S693 (2003)
- [8] J. H. Dil, *J. Phys.: Cond. Mat.* **21**, 403001 (2009)
- [9] D. Huertas-Hernando, F. Guinea, A. Brataas, *Phys. Rev. B* **74**, 155426 (2006)
- [10] K. Sugawara, T. Sato, S. Souma, T. Takahashi, M. Arai, and T. Sasaki, *Phys. Rev. Lett.* **96**, 046411 (2006)
- [11] D. Hsieh, Y. Xia, L. Wray, D. Qian, A. Pal, J. H. Dil, J. Osterwalder, F. Meier, G. Bihlmayer, C. L. Kane, Y. S. Hor, R. J. Cava, M. Z. Hasan, *Science* **323**, 919 (2009)
- [12] Y. Liu and R. E. Allen, *Phys. Rev. B* **52**, 1566 (1995) and references therein
- [13] C. R. Ast, H. Höchst, *Phys. Rev. Lett.* **87**, 177602 (2001)
- [14] Y. M. Koroteev, G. Bihlmayer, J. E. Gayone, E. V. Chulkov, S. Blügel, P. M. Echenique, P. Hofmann, *Phys. Rev. Lett.* **93**, 046403 (2004)
- [15] F. Kuemmeth, S. Ilani, D. C. Ralph, and P. L. McEuen, *Nature* **452**, 448 (2008)
- [16] J.-S. Jeong, H.-W. Lee, *Phys. Rev. B* **80**, 075409 (2009)
- [17] D. Pacilé, C. R. Ast, M. Papagno, C. Da Silva, L. Moreschini, M. Falub, A. P. Seitsonen and M. Grioni *Phys. Rev. B* **73** 245429 (2006)
- [18] C. R. Ast, J. Henk, A. Ernst, L. Moreschini, M. C. Falub, D. Pacilé, P. Bruno, K. Kern and M. Grioni *Phys. Rev. Lett.* **98** 186807 (2007)
- [19] C. R. Ast, D. Pacilé, L. Moreschini, M. C. Falub, M. Papagno, K. Kern, M. Grioni, J. Henk, A. Ernst, S. Ostanin and P. Bruno, *Phys. Rev. B* **77**, 081407 (R) (2008)
- [20] L. Moreschini, A. Bendounan, I. Gierz, C. R. Ast, H. Mirhosseini, H. Höchst, K. Kern, J. Henk, A. Ernst, S. Ostanin, F. Reinert and M. Grioni, *Phys. Rev. B* **79** 075424 (2009)
- [21] L. Moreschini, A. Bendounan, H. Bentmann, M. Assig, K. Kern, F. Reinert, J. Henk, C. R. Ast and M. Grioni *Phys. Rev. B* **80** 035438 (2009)
- [22] A. Barbieri and M. A. Van Hove, Symmetrized Automated Tensor LEED package, available from M. A. Van Hove
- [23] A. Barbieri and M. A. Van Hove, private communication
- [24] J. B. Pendry, *J. Phys. C: Solid St. Phys.* **13**, 937 (1980)
- [25] J. Dalmas, H. Oughaddou, C. Léandri, J.-M. Gay, G. Le Lay, G. Tréglia, B. Aufray, O. Bunk and R. L. Johnson *Phys. Rev. B* **72** 155424 (2005)
- [26] S. Oppo, V. Fiorentini, and M. Scheffler, *Phys. Rev. Lett.* **71**, 2437 (1993)
- [27] D. P. Woodruff and J. Robinson *J. Phys.: Condens. Matter* **12** 7699 (2000)
- [28] E. A. Soares, C. Bittencourt, V. B. Nascimento, V. E. de Carvalho, C. M. C. de Castilho, C. F. McConville, A. V. de Carvalho, D. P. Woodruff *Phys. Rev. B* **61** 13983 (2000)
- [29] P. D. Quinn, D. Brown, D. P. Woodruff, P. Bailey and T. C. Q. Noakes *Surf. Science* **511** 43 (2002)
- [30] T. Hirahara, T. Komorida, A. Sato, G. Bihlmayer, E. V. Chulkov, K. He, I. Matsuda and S. Hasegawa *Phys. Rev. B* **78** 035408 (2008)
- [31] C. R. Ast, G. Wittich, P. Wahl, R. Vogelgesang, D. Pacilé, M. C. Falub, L. Moreschini, M. Papagno, M. Grioni, and K. Kern, *Phys. Rev. B* **75**, 201401 (R) (2007)
- [32] F. Meier, H. Dil, J. Lobo-Checa, L. Patthey and J. Osterwalder *Phys. Rev. B* **77** 165431 (2008)
- [33] F. Meier, V. Petrov, S. Guerrero, C. Mudry, L. Patthey, J. Osterwalder, J. H. Dil, *Phys. Rev. B* **79**, 241408 (R) (2009)
- [34] S. A. de Vries, W. J. Huisman, P. Goettkindt, M. J. Zwanenburg, S. L. Bennett, I. K. Robinson and E. Vlieg *Surf. Science* **414** 159 (1998)
- [35] P. Bailey, T. C. Q. Noakes, D. P. Woodruff, *Surf. Sci.* **426**, 358 (1999)
- [36] F. Meier, V. Petrov, H. Mirhosseini, L. Patthey, J. Henk, J. Osterwalder, and J. Hugo Dil, arXiv:1001.4927 (2010)
- [37] D. Kaminski, P. Poodt, E. Aret, N. Radenovic, E. Vlieg, *Surf. Sci.* **575**, 233 (2005)
- [38] H. Bentmann, F. Forster, G. Bihlmayer, E. V. Chulkov, L. Moreschini, M. Grioni and F. Reinert, *Europhys. Lett.* **87**, 37003 (2009)
- [39] This results from explicitly considering the lattice constant in the tight-binding calculation presented in Ref. 4.
- [40] These values are estimated as an upper limit from the line width in the momentum distribution of the experimental band structure in Sb/Cu(111).
- [41] H. Mirhosseini, J. Henk, A. Ernst, S. Ostanin, C.-T. Chiang, P. Yu, A. Winkelmann, and J. Kirschner, *Phys. Rev. B* **79**, 245428 (2009)
- [42] H. Cercellier, C. Didiot, Y. Fagot-Revurat, B. Kierren, L. Moreau, and D. Malterre, and F. Reinert, *Phys. Rev. B* **73**, 195413 (2006)
- [43] As we expect the spin-splitting in the Cu(111) surface state to be smaller than for the Ag(111) surface state, we have set the values to zero for the purpose of this work.